Molecular Therapy
Original Article

Increased Survival by Pulmonary Treatment of Established Lung Metastases with Dual STAT3/CXCR4 Inhibition by siRNA Nanoemulsions

Zhaoting Li,[1] Gang Chen,[1,3] Ling Ding,[1,2] Yixin Wang,[1] Chenfei Zhu,[1] Kaikai Wang,[1,4] Jing Li,[2] Minjie Sun,[1] and David Oupicky[2]

[1]State Key Laboratory of Natural Medicines, Department of Pharmaceutics, China Pharmaceutical University, Nanjing 210009, China; [2]Center for Drug Delivery and Nanomedicine, Department of Pharmaceutical Sciences, University of Nebraska Medical Center, Omaha, NE 68198, USA

Lung metastasis is a common and deadly occurrence in many types of solid tumors. Chemokine receptor CXCR4 and transcription factor signal transducer and activator of transcription 3 (STAT3) are among potential therapeutic targets in lung metastatic cancer. Both CXCR4 and STAT3 play important roles in the proliferation, angiogenesis, and metastasis of cancer cells. Here, we report on the development of a pulmonary delivery (p.d.) system based on perfluorocarbon (PFC) nanoemulsions for combined delivery of a partially fluorinated polymeric CXCR4 antagonist (FM) and anti-STAT3 small interfering RNA (siRNA). We have prepared FM-stabilized PFC (FM@PFC) as a delivery system of therapeutic siRNA adsorbed on the surface of the emulsion. These FM@PFC/siRNA nanoemulsions inhibited both CXCR4 and STAT3, as demonstrated by effective anti-invasive ability *in vitro* and related antimetastatic activity *in vivo*. The combined nanoemulsions provided a comprehensive anticancer effect in the model of established lung metastasis of breast carcinoma, which was dependent on induction of cancer cell apoptosis, anti-angiogenic effect, anti-invasive activity, and overcoming of the immunosuppressive tumor microenvironment. Direct comparison with intravenous (i.v.) injection showed superior activity of pulmonary administration as indicated by significantly increased animal survival. Overall, this work established the suitability of the PFC nanoemulsions for p.d. of combination anticancer treatments and as a promising method to treat lung metastasis.

INTRODUCTION

The vast majority of deaths caused by solid cancers is the result of metastatic spread of the primary disease.[1] Lung metastasis is a common occurrence and lethal determinant in many cancers. The most common primary tumors in adults that metastasize to the lungs include breast cancer, renal cell carcinoma, colon cancer, and head and neck cancer. In the pediatric population, the most common primary tumors that develop lung metastases are osteosarcoma, rhabdomyosarcoma, and Ewing sarcoma.[2–5] Despite the efforts in the development of better therapies, progress in the treatment of advanced pulmonary metastatic disease remains limited.

Direct pulmonary delivery (p.d.) emerged as an attractive approach to treat lung metastases due to the direct access to the disease site and minimization of the systemic exposure in patients subjected to prior or concurrent systemic chemotherapy.[6,7] Multiple types of delivery vectors showed promise in the treatment of both lung metastasis and primary lung cancer. For example, codelivery of a chemotherapy doxorubicin and anti-Bcl-2 small interfering RNA (siRNA) to the lungs provided a local treatment strategy for lung cancer.[8] In lung metastatic melanoma and Lewis lung carcinoma, intratracheal administration of therapeutic siRNA by cationic lipid particles showed promising activity.[9] p.d. provides enhanced retention of the active ingredients in the lungs and decreased absorption into the systemic circulation, making it suitable for the treatment of advanced lung metastasis.

The process of metastasis is complex and involves various factors, including multiple chemokines and chemokine receptors that are responsible for cancer cell migration and invasion. CXCR4 is a prominent chemokine receptor that, together with its ligand CXCL12, plays a crucial role in breast cancer metastasis to the lung.[10,11] CXCR4 activation leads to the initiation of multiple signaling pathways that regulate cell adhesion, invasion, angiogenesis, and proliferation.[12,13] Recent evidence also shows that CXCR4 inhibition decreases tumor fibrosis, increases T cell infiltration, and helps to overcome immunosuppression in metastatic breast cancer models, suggesting the

Received 31 May 2019; accepted 14 August 2019;
https://doi.org/10.1016/j.ymthe.2019.08.008.

[3]Present address: Institute of Comparative Medicine, College of Veterinary Medicine, Yangzhou University, Yangzhou 225009, China.

[4]Present address: School of Pharmacy, Nantong University, Nantong 226001, China.

Correspondence: David Oupicky, Center for Drug Delivery and Nanomedicine, Department of Pharmaceutical Sciences, University of Nebraska Medical Center, Omaha, NE 68198, USA.
E-mail: david.oupicky@unmc.edu

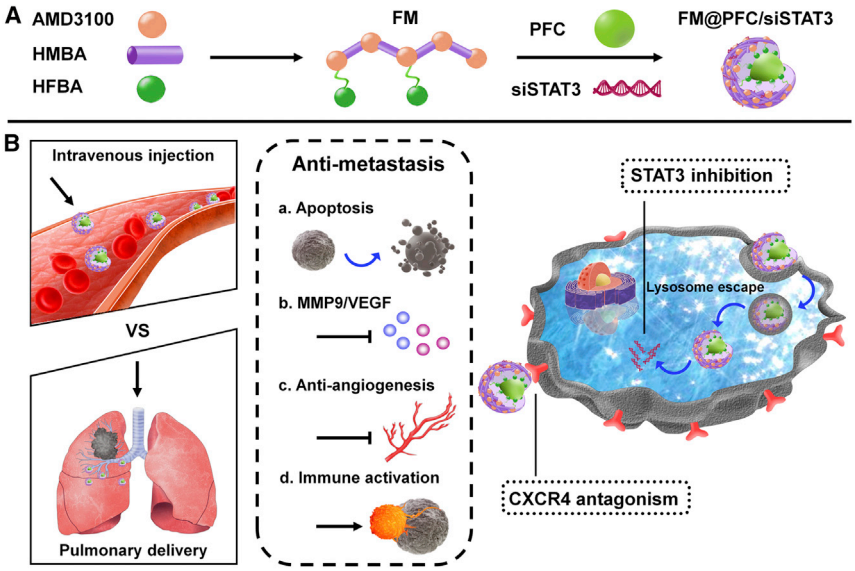

Figure 1. Preparation and Mechanism of Action of the FM@PFC/siSTAT3 Nanoemulsions

(A) Michael-addition copolymerization of AMD3100 with HMBA resulted in the formation of M, which was subsequently fluorinated with HFBA to obtain FM. PFC nanoemulsion was stabilized with FM through fluorous interactions before loading siSTAT3 by electrostatic adsorption. (B) Treatment with FM@PFC/siSTAT3 inhibits CXCR4 and silences expression of STAT3 to inhibit tumor metastasis by promoting apoptosis, decreasing MMP9/VEGF expression, blocking tumor neovascularization, and activating antitumor immunity in the tumor microenvironment.

CXCR4 axis as a promising target for combined immunotherapy strategies.[14,15]

Signal transducer and activator of transcription 3 (STAT3) is a transcription factor that provides important support for the proliferation of cancer cells and metastasis. Activated STAT3 regulates the function of many non-transformed cells that affect metastatic sites and constitute the tumor microenvironment. Specifically, STAT3 is involved in the infiltration and activation of immunosuppressive cells, such as T-regulatory cells (Tregs), T helper 17 cells, and myeloid-derived suppressor cells (MDSCs).[16–18] STAT3 induces the expression of various cytokines, growth factors, and pro-angiogenic factors, whose receptors then in turn activate STAT3 in a feed-forward loop between cancer cells and immune cells in the tumor microenvironment.[19–21] Thus, activation of STAT3 contributes both to the tumor-promoting inflammation and the suppression of anti-tumor immunity. Persistent activation of STAT3 is associated with malignant properties,[22,23] which makes it an attractive target for cancer therapy. Combining CXCR4 and STAT3 inhibition is a promising approach for antimetastatic and tumor immune microenvironment-modulating therapies.

We have previously reported the development of fluorinated polycations with enhanced cell association and gene transfection efficacy.[24,25] In the present study, we aimed to investigate a fluorinated polymer with CXCR4 antagonist properties, named FM, as a vector for pulmonary siRNA delivery in advanced lung metastatic disease. To that end, we have prepared perfluorocarbon (PFC) nanoemulsions stabilized with FM as a functional vector for p.d. of therapeutic STAT3-silencing siRNA (siSTAT3) (Figure 1A). CXCR4 and STAT3 are closely involved in the formation of lung metastasis, and we have previously reported that p.d. of CXCR4 and STAT3 combined inhibitors achieved good anti-lung metastasis efficacy in osteosarcoma.[26] Here, we further expanded the use of this treatment strategy to pulmonary metastases of different origin (breast cancer) and conducted direct head-to-head comparison of p.d. with intravenous (i.v.) treatment using the same therapeutic targets (Figure 1B). This study clearly demonstrates the benefits of local p.d. treatment when compared with the i.v. administration. The FM-stabilized PFC (FM@PFC) nanoemulsion opens up the opportunity and establishes a therapeutic pulmonary siRNA delivery nanoplatform for the treatment of advanced lung metastasis.

RESULTS

Preparation and Characterization of Nanoemulsions

We have previously developed CXCR4 antagonistic polycations for delivery of therapeutic nucleic acids.[24,27,28] Here, we have used polycations based on commercial CXCR4 antagonist AMD3100 (PAMD), which were fluorinated by reaction with heptafluorobutyric anhydride as before to obtain F-PAMD.[24] The resultant polymer, which will for simplicity be named FM in this study, had molecular weight 13.5 kDa and contained 5 weight % fluorine (Figure S1). We used FM as a stabilizer at the surface and perfluorodecalin as an emulsion core following a similar approach described in our recent studies.[26] The approach utilizes the high-affinity fluorous interactions between PFC and the heptafluorobutyryl moieties in FM for coating and stabilization of the FM@PFC. The hydrodynamic diameter of the prepared FM@PFC was ~200 nm with a polydispersity index of 0.109 (Figure 2A). The zeta potential of the FM@PFC was highly positive 53 mV (Figure 2C), and the emulsions presented as regular spherical structures in the transmission electron microscopy (TEM) (Figure 2B).

The highly positive surface charge of the FM@PFC was then used to bind siRNA to form nanoemulsion FM@PFC/siRNA as validated by a gel retardation assay (Figure 2E). In this study, we compared the nanoemulsions with polycation/siRNA polyplexes prepared with either fluorinated F-PAMD (FM) or the non-fluorinated parent PAMD (M). The FM@PFC showed similar siRNA binding ability as M and FM when considering only the content of the M. Binding of the siRNA to the emulsion (M/siRNA w/w = 2) decreased zeta potential to ~28 mV and slightly decreased the hydrodynamic diameter

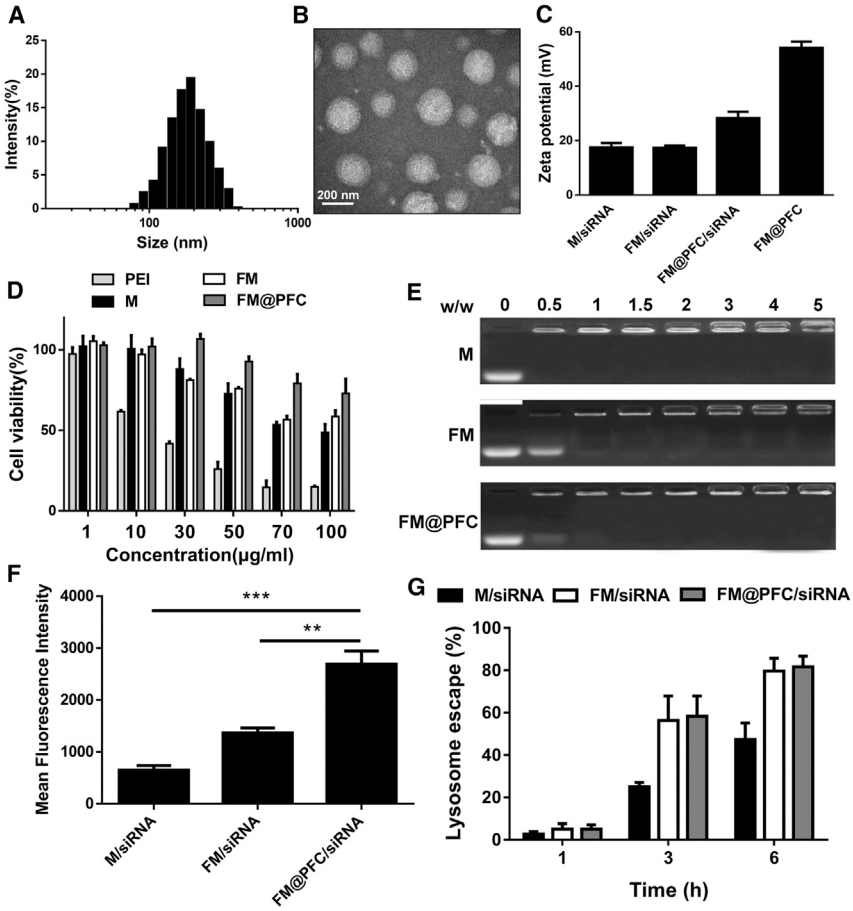

Figure 2. Physicochemical Characterization of FM@PFC/siRNA Nanoemulsions

(A) Hydrodynamic size distribution of FM@PFC. (B) TEM of FM@PFC. (C) Zeta potential of the formulations (polymer/siRNA w/w ratio 2). (D) Cytotoxicity of PEI, M, FM, and FM@PFC in L929 cells. (E) Agarose gel retardation assay at varying M/siRNA w/w ratios. (F) Cell association of polyplexes (M/siRNA and FM/siRNA) and nanoemulsions (FM@PFC/siRNA) analyzed by flow cytometry in 4T1.Luc cells after 4 h incubation with the formulations prepared with FAM-siRNA at w/w ratio 2 (siRNA 100 nM). Data are presented as the mean ± SD with unpaired t test, $n \geq 3$, $^{**}p < 0.01$, $^{***}p < 0.001$. (G) Extent of endosomal escape at 1–6 h.

to ~190 nm with polydispersity index of 0.117 (Figure S2). We then evaluated the initial cytotoxicity of the polymers in mouse fibroblasts L929 (Figure 2D). We found that fluorination alone had no significant effect on cytotoxicity and both FM and FM@PFC showed lower cytotoxicity when compared with a benchmark 25 kDa PEI.

Intracellular Trafficking and Gene Silencing

We evaluated cell association and intracellular trafficking of the nanoemulsions formulated with fluorescently labeled siRNA in 4T1 breast cancer cells stably expressing luciferase (4T1.Luc). The cell association of the FM@PFC/siRNA nanoemulsion was higher than the FM/siRNA polyplexes, which exceeded the cell association of non-fluorinated M/siRNA polyplexes (Figure 2F). Endosomal escape is a notorious bottleneck for intracellular delivery of polyplexes.[29] Confocal microscopy analysis found that 1 h after incubation, the majority of the endocytosed siRNA (green) was localized in LysoTracker-positive vesicles (Figure 2G). However, endosomal escape of the siRNA was evident as early as 3 h after incubation and further increased at 6 h.

We next validated the ability of the nanoemulsions to silence the Luc reporter gene expression in 4T1.Luc cells. FM/siLuc polyplexes showed better silencing ability than M/siLuc polyplexes, thus confirming beneficial effects of fluorination on increasing polyplex transfection. With incorporation of FM into emulsions, the FM@PFC/siLuc showed the best Luc gene silencing ability of all the tested samples (Figure 3A). Taken together, FM@PFC/siRNA nanoemulsions can enter the cancer cells and facilitate efficient endosomal escape.

Anticancer and Anti-invasive Activity of Nanoemulsions

In Figure 3B, we found that blocking CXCR4 with the polyplexes inhibited the colony formation of 4T1.Luc cells and the number of colonies was the lowest after the FM@PFC/siSTAT3 treatment. As shown in Figure 3C, FM@PFC/siSTAT3 inhibited 4T1.Luc cell growth more effectively than both M/siSTAT3 and FM/siSTAT3. The detection of apoptotic cells using Annexin V and propidium iodide (PI) staining showed significantly more apoptosis following treatment with FM/siSTAT3 than with M/siSTAT3. Importantly, less apoptosis was seen in the FM/siSTAT3-treated cells than in cells treated with FM@PFC/siSTAT3 (Figure 3D), most likely because of better cell association and siRNA transfection efficiency.

We evaluated anti-invasive activity of FM@PFC/siSTAT3 in transwell cell migration and invasion assays. Both CXCR4 and STAT3 play important roles in promoting cancer cell migration and invasion, which are needed for metastatic spread. We used CXCL12 as a chemoattractant with CXCR4-overexpressing osteosarcoma U2OS cells. As shown in Figure 3E, at 2.5 μg/mL, all tested samples showed effective and comparable inhibition of cell invasion as the positive control AMD3100 (0.15 μg/mL). To investigate how the combination of CXCR4 antagonism and STAT3 gene silencing affected the cell invasion, we used fetal bovine serum (FBS) as a broad chemoattractant. As expected, FM@PFC/scrambled siRNA (siScr) showed limited ability to inhibit cell migration due to its CXCR4 specificity. In contrast, combined treatment with FM@PFC/siSTAT3 decreased cell invasion by 79%, which was significantly higher than other tested formulations

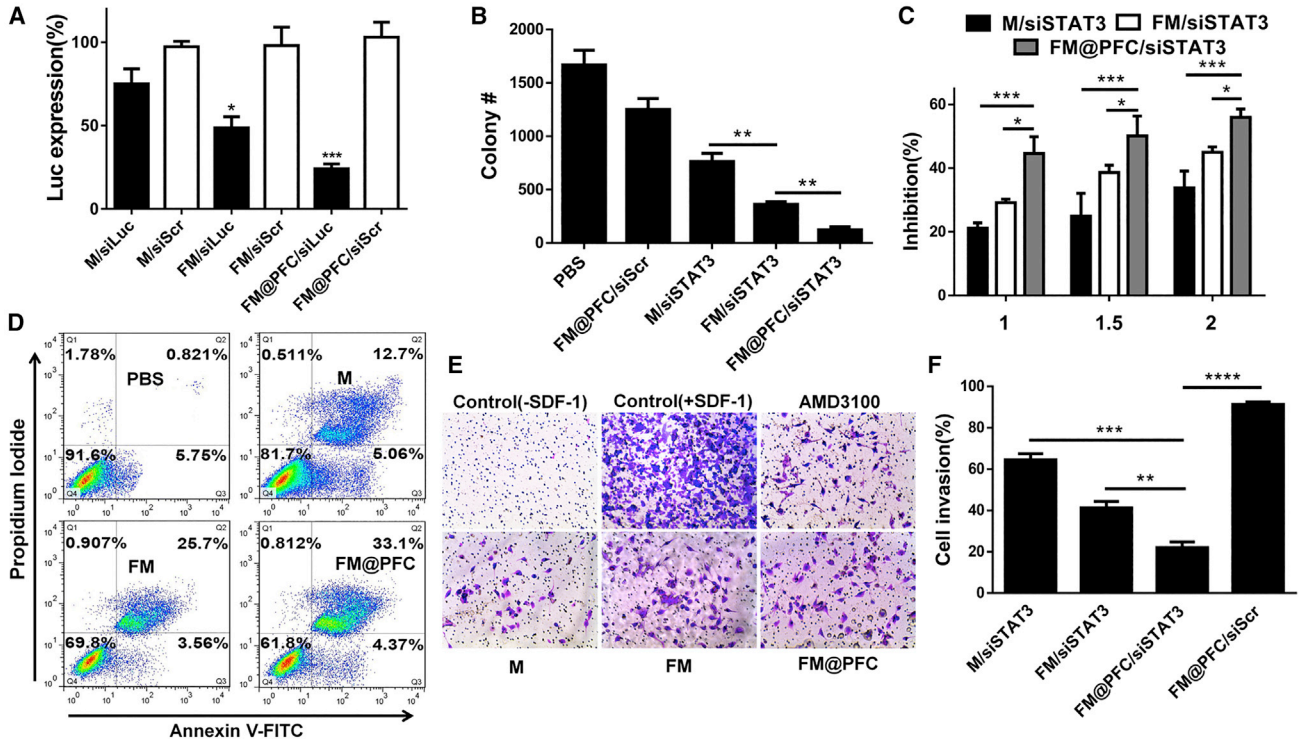

Figure 3. Anti-cancer Efficacy of FM@PFC/siSTAT3 Nanoemulsions *In Vitro*

(A) Luciferase silencing in 4T1.Luc cells using formulations at w/w 2 (siLuc 100 nM). Cells were treated with the formulations prepared with control siScr or siLuc. Data presented as the mean ± SD with unpaired t test, $n \geq 3$, *$p < 0.05$, ***$p < 0.001$ versus M/siLuc. (B) Colony formation after treatment. (C) Cell growth inhibition of 4T1.Luc cells. Statistical comparisons by two-way ANOVA with Tukey's multiple comparisons test. (D) Induction of apoptosis by the formulations with siSTAT3 in 4T1.Luc cells. Annexin V-positive cells in quadrants 2 and 3 of the flow cytometry plot were considered apoptotic. Inhibition of cell invasion using (E) human U2OS osteosarcoma cells and (F) mouse 4T1.Luc. The cells were treated with M, FM, FM@PFC or the corresponding siSTAT3 formulations, and AMD3100 (300 nM) and allowed to invade through a layer of Matrigel upon stimulation with SDF-1 (U2OS) or FBS (4T1.Luc). Data are presented as the mean ± SD with unpaired t test, $n \geq 3$, *$p < 0.05$, **$p < 0.01$, ***$p < 0.001$, ****$p < 0.0001$.

with siSTAT3: FM/siSTAT3 (~60%) and M/siSTAT3 (~36%) (Figure 3F).

Biodistribution

Biodistribution was evaluated by whole-body fluorescence imaging using polyplexes prepared with Cy5-labeled siRNA (Figure 4A) and administered either by p.d. using intratracheal instillation or by i.v. injection. At 1 h after administration, both the FM/siRNA (Figure 4C) and FM@PFC/siRNA (Figures 4D and 4E) in the p.d. group were mainly concentrated in the lungs, but the FM/siRNA polyplexes in the i.v. injection group showed very low lung accumulation. Most of the siRNA in the i.v. group was rapidly cleared by the kidneys, suggesting poor plasma stability of the FM/siRNA polyplexes and their dissociation at the glomerular basement membrane. At 12 and 24 h, the p.d. group retained a good amount of siRNA in the lung, but the i.v. group showed a negligible amount of pulmonary distribution, with most of the fluorescence found in the liver and kidneys. The higher concentration of the siRNA and the more favorable distribution to the lung metastases (Figure 4B) was expected to lead to improved efficacy in the subsequent studies.

Effect of the Administration Route on Antimetastatic Activity

Antimetastatic activity of the FM@PFC/siSTAT3 nanoemulsions was investigated in an experimental lung metastasis model of breast cancer. The lung metastases were established by i.v. injection of 4T1.Luc cells in BALB/c mice. Animals with detectable lung metastases were treated either by p.d. via intratracheal instillation or by tail vein injection. The treatments were given on days 7, 9, 11, and 13, and the animals were sacrificed on day 15 to compare the efficacy of the two methods of administration. The anticancer activity of formulations given by p.d. was significantly better than with the i.v. treatment based on the measurement of lung tumor burden using total bioluminescence signal of the 4T1.Luc cells (Figure 5A). Moreover, FM@PFC/siSTAT3 was more efficacious than FM/siSTAT3, likely because of increased transfection efficacy. The differences in the number of detected surface lung metastases confirmed superior antineoplastic effect of p.d. of FM@PFC/siSTAT3 (Figure 5B). H&E staining of the lungs showed the presence of metastases and validated the best antimetastatic effect of the FM@PFC/siSTAT3 p.d. treatment group (Figure 5C). The number and size of metastases in the FM/siSTAT3 p.d. group were significantly lower

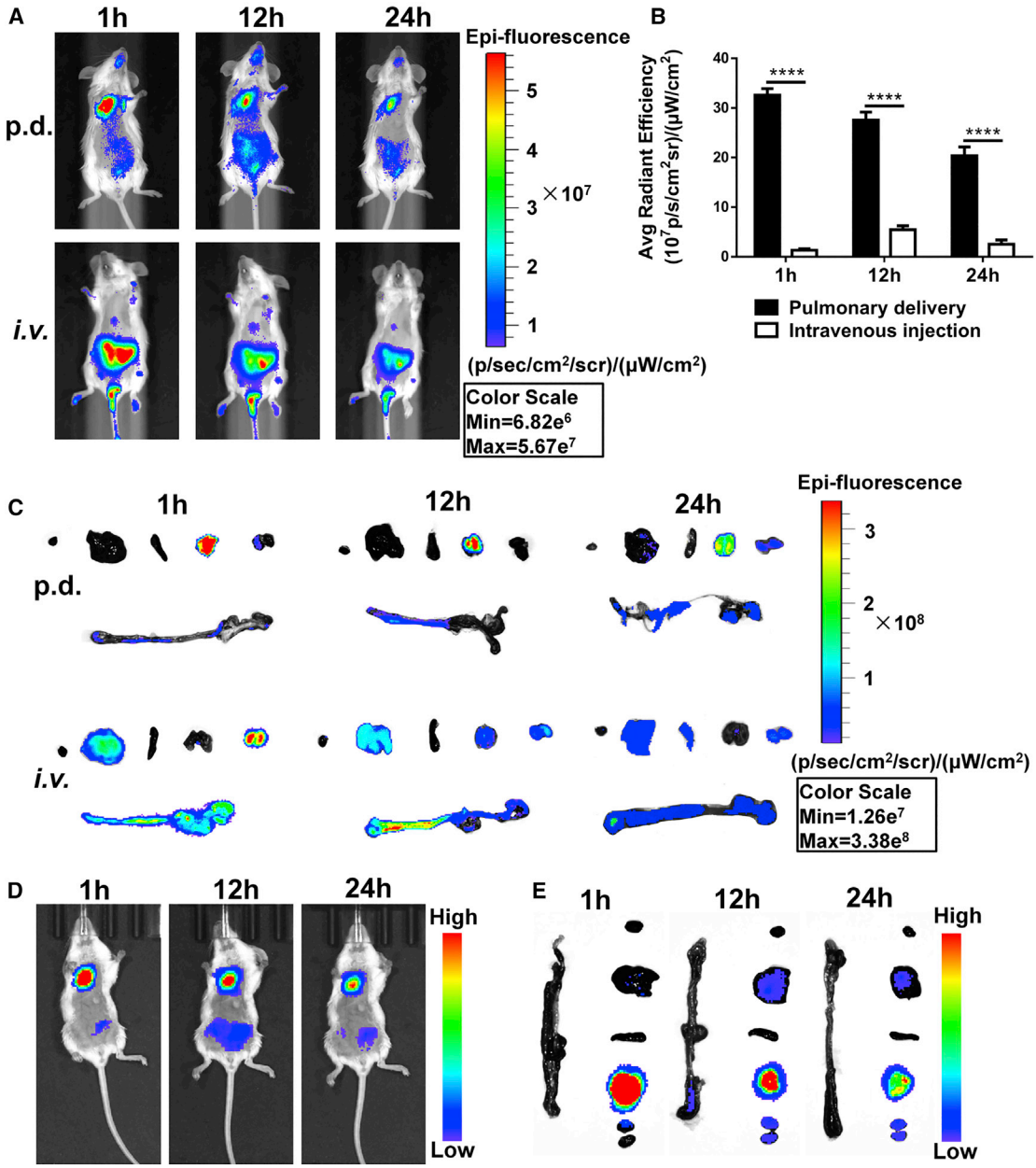

Figure 4. Biodistribution of Cy5-siRNA Polyplexes and Nanoemulsions *In Vivo*

(A) *In vivo* fluorescence images at different times after p.d. and i.v. injection of the polyplexes (1.2 mg/kg Cy5-siRNA, w/w 2). (B) Relative lung distribution of siRNA-Cy5 based on *ex vivo* fluorescence intensity after p.d. or i.v. injection of the polyplexes (mean ± SD, unpaired t test, n = 3), ****$p < 0.0001$. (C) *Ex vivo* siRNA-Cy5 fluorescence images of major organs after p.d. or i.v. administration. From left to right: heart, liver, spleen, lung, kidneys, and intestines. (D) *In vivo* fluorescence images after p.d. of the Cy5-siRNA nanoemulsions (1.2 mg/kg Cy5-siRNA, w/w 2). (E) *Ex vivo* siRNA-Cy5 fluorescence images of major organs after p.d. of the nanoemulsions. From top to bottom: heart, liver, spleen, lung, kidney, and intestines.

than in the FM/siSTAT3 i.v. injection treated group demonstrating the superiority of p.d.

Survival is the ultimate endpoint used to evaluate anticancer efficacy. We thus treated the mice on days 7, 9, 11, 13, 15, and 17 and monitored survival for up to 50 days (Figure 5D). As expected, the FM@PFC/siSTAT3 p.d. treatment showed the best activity with a median survival of 49 days (versus 22 days for untreated animals). Half of the mice survived until the end of the experiment on day 50. The p.d. of the FM/siSTAT3 polyplexes also prolonged the survival

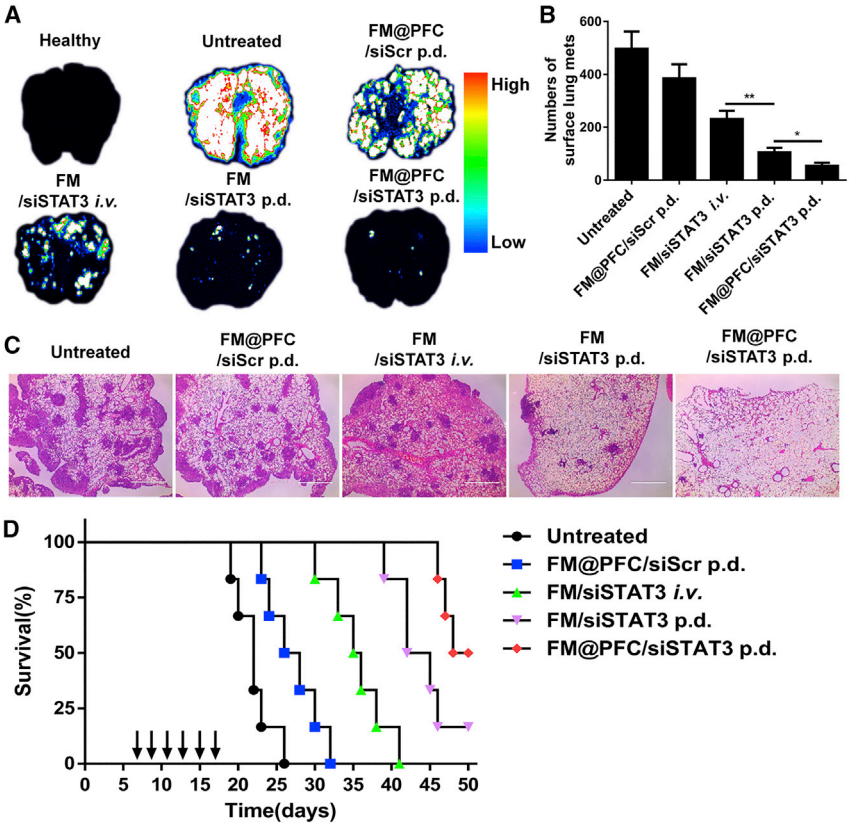

Figure 5. Antimetastasis Efficacy of FM@PFC/siRNA Nanoemulsions *In Vivo*

(A) Bioluminescence images of whole lungs with 4T1.Luc tumors on day 15. The formulations were administered by p.d. or i.v. injection on days 7, 9, 11, and 13. (B) Numbers of surface lung metastases after different treatments on day 15. (C) H&E staining of the lung metastasis after different treatments (scale bar equals 1 mm). (D) Effect of treatment on animal survival (n = 6). Log-rank test: FM@PFC/siSTAT3 p.d. versus FM@PFC/siScr p.d. (p = 0.0005); FM/siSTAT3 p.d. versus FM/siSTAT3 i.v. (p = 0.0016). (Median survival: untreated 22 days; FM@PFC/siScr p.d., 27 days; FM/siSTAT3 i.v., 35.5 days; FM/siSTAT3 p.d., 43 days; FM@PFC/siSTAT3 p.d., 49 days).

significantly more than the comparable i.v. treatment as indicated by the median survival of 43 days versus 35.5 days for the i.v. injection (log-rank test: p = 0.0016). The lower activity of the FM/siSTAT3 polyplexes versus FM@PFC/siSTAT3 nanoemulsions points to the benefits of the nanoemulsions in p.d. with enhanced tumor cell association and gene transfection efficacy. Even a formulation with CXCR4 inhibition only (FM@PFC/siScr p.d.) prolonged the median survival from the 22 days (untreated) to 27 days (log-rank test: p = 0.0126), indicating that blocking CXCR4 is helpful for prolonging the survival in the established lung metastasis model of breast cancer.

Mechanism of Antimetastatic Activity of FM@PFC/siSTAT3

The above results showed that FM@PFC/siSTAT3 exerts its antimetastatic effect in a relatively broad manner. In order to comprehend the mechanism of action, we studied the modulation of key signaling pathways in 4T1.Luc cells. Treatment with FM@PFC/siSTAT3 showed a greater inhibition of STAT3 expression and subsequent decrease in the content of the activated phosphorylated STAT3 (p-STAT3) than FM/siSTAT3 and M/siSTAT3 (Figure 6A). Pro-apoptotic effects of the treatments were assessed by measuring the expression of Bcl-2 and pERK. FM@PFC/siSTAT3 downregulated the expression of both Bcl-2 and pErk significantly more than FM/siSTAT3 and M/siSTAT3. FM@PFC/siSTAT3 upregulated E-cadherin expression to an extent that was larger than the control FM/siSTAT3 and M/siSTAT3.

To explore the antimetastasis mechanism of the FM@PFC/siSTAT3 nanoemulsions *in vivo*, the tumor microenvironment was analyzed with immunohistochemistry and immunofluorescence. We validated that the nanoemulsions silence the expression of STAT3 and subsequently decrease the levels of the activated form of STAT3 (p-STAT3). The FM@PFC/siSTAT3 given by p.d. showed the most effective STAT3 gene silencing of all the tested treatments (Figure 6B). The activated form of STAT3 (p-STAT3) is important for promoting anti-apoptotic activity in tumor cells through B cell lymphoma-extra large (BCL-XL) and tumor angiogenesis through the induction of pro-angiogenic factors such as vascular endothelial growth factor (VEGF), hepatocyte growth factor (HGF), fibroblast growth factor (bFGF), matrix metalloproteinase 2 (MMP2), and MMP9.[19,21,30,31] We have shown above that the nanoemulsions downregulate the expression of Bcl-2 and thus we further explored their effect on the expression of MMP9 and VEGF *in vivo*. FM@PFC/siSTAT3 p.d. group showed a better effect than the FM/siSTAT3 i.v. and FM/siSTAT3 p.d. groups (Figure 6C). VEGF expression decreased more in the FM@PFC/siSTAT3 p.d. group than in the FM/siSTAT3 i.v. group and the FM/siSTAT3 p.d. group. Consistent with the MMP9 and VEGF data, the CD31 expression in FM@PFC/siSTAT3 group was the lowest, proving that FM@PFC/siSTAT3 can inhibit tumor neovascularization. The Ki67 staining showed that the FM/siSTAT3 p.d. treatment inhibited the metastasis growth significantly better than the FM/siSTAT3 i.v. treatment and the FM@PFC/siSTAT3 treatment showed the best growth inhibition (Figure 6D).

Increased STAT3 activity in tumors influences the expression of immune-stimulating factors and contributes to immune suppression and tumor evasion.[32] To test the hypothesis that our treatment contributes to overcoming tumor immunosuppression, we measured the infiltration of $CD8^+$ T cells in the lung metastasis. As shown in Figure 6E, there was more infiltration of $CD8^+$ T cells in FM@PFC/siSTAT3 p.d.-treated mice than in mice treated with FM/siSTAT3 i.v. and FM/siSTAT3 p.d. Interestingly, we found that silencing STAT3

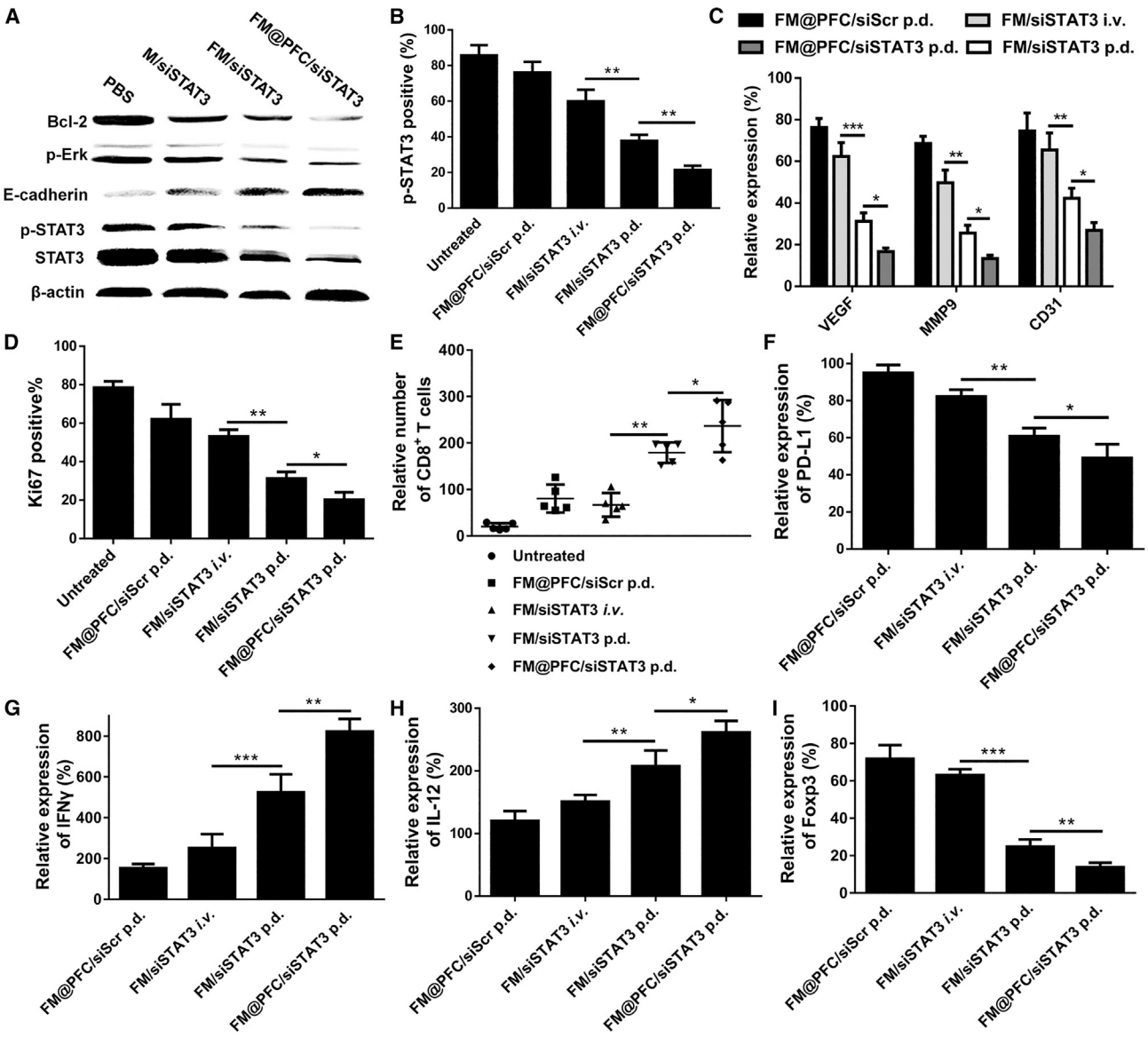

Figure 6. Mechanism of Action of FM@PFC/siSTAT3 Nanoemulsions

(A) Western blot analysis for Bcl-2, pERK, E-cadherin, p-STAT3, and STAT3 in 4T1.Luc cells treated with different formulations prepared at polymer/siRNA w/w ratio 2 (siSTAT3 100 nM). (B) Analysis of immunohistochemistry staining of p-STAT3 in lung metastasis. (C) Relative expression of VEGF, MMP9, and CD31 in lung metastasis. (D) Ki67 positive% in the lung metastasis. (E) $CD8^+$ T cells infiltration in lung metastasis. Relative (F) PD-L1, (G) IFN-γ, (H) IL-12, and (I) Foxp3 expression in lung metastasis. Semiquantitation of the staining was made with ImagePro Plus. Data are presented as the mean ± SD, n = 3, unpaired t test, *$p < 0.05$, **$p < 0.01$, ***$p < 0.001$.

expression can decrease the programmed death-ligand 1 (PD-L1) expression in the lung metastases and blocking CXCR4 can increase CD8 T cell infiltration, which should enhance the anti-tumor immune effect (Figure 6F). Correspondingly, significantly elevated levels of interferon-γ (IFN-γ) and interleukin-12 (IL-12) were observed in the FM@PFC/siSTAT3 p.d. group than in the FM/siSTAT3 i.v. and FM/siSTAT3 p.d. groups (Figures 6G and 6H), indicating that p.d. activates the antitumor immune response more efficiently than comparable i.v. delivery. Expression of Foxp3, a marker for detection of Tregs, contributes to acquisition of immune-suppressive tumor properties.[33,34] As shown in Figure 6I, the expression of Foxp3 decreased the most with the treatment of FM@PFC/siSTAT3 p.d. confirming the favorable effect of our treatment in overcoming the tumor immunosuppressive environment.

DISCUSSION

Despite significant advances in diagnosis and treatment, lung metastasis persists as a barrier to successful therapy and remains as a

main cause of cancer-related deaths. During the formation and growth of lung metastasis, the tumor cells closely interact with the surrounding microenvironment. The tumor cells control the microenvironment by releasing extracellular signals that contribute to angiogenesis induction of immune tolerance. MMP9 induction by VEGF receptor is involved in lung-specific metastasis and potentiates metastasis formation.[35,36] In this study, we showed that the FM@PFC/siSTAT3 inhibited tumor cell growth, reduced colony formation, and promoted apoptosis through combined inhibition of CXCR4 and STAT3. We found that FM@PFC/siSTAT3 downregulated the Bcl-2, pERK, and Ki67 expression to inhibit the metastasis growth and reduced the VEGF and MMP9 expression to inhibit tumor angiogenesis

In the process of tumorigenesis, STAT3 activation is a survival mechanism of many different types of cancer cells, which makes STAT3 inhibition a promising strategy for cancer treatment.[18,37,38] STAT3 activation is also an immunoregulatory mechanism, which changes the balance of cytokines from anti-tumor IL-12 (activation of natural killer cells and effector T cells) to oncogenic IL-23 (which activates Tregs) in tumorigenesis. However, only relieving the immunosuppressive state in the microenvironment of tumor immunity may not kill tumor cells effectively. Potent anti-tumor immune response requires sufficient amount of effector T cells. We demonstrated that the FM@PFC/siSTAT3 treatment increased the IL-12 expression and decreased the Foxp3 (a specific marker of Tregs) expression in the tumor metastasis to transform the immunosuppression state into an immune activation state in the metastasis microenvironment. Previous reports have shown that STAT3 drives PD-L1 expression.[39,40] We found that STAT3 inhibition in the breast cancer lung metastasis downregulated the PD-L1 expression, which further relieved the immunosuppression and activated effector T cells. There have been many successful cases of anti-PD-L1 immunotherapy in the treatment of preclinical models and cancer patients. However, its efficacy in metastatic triple-negative breast cancer is limited. Insufficient T cell infiltration has compromised the anti-tumor immunity brought by PD-L1 inhibition.[41,42] Notably, our data suggested that CXCR4 antagonism by the FM@PFC increased the CD8 T cells infiltration in the lung metastasis, which enhanced the STAT3- and PD-L1-related effects.

Treatment of lung metastases is dependent on the adequate distribution of the therapeutic agents to the metastatic target lesions. PFCs have been widely used in oxygen delivery, ultrasound imaging, organ transplantation, and prevention of ischemia reperfusion tissue injury.[43–46] Here, the fluorinated polycations were used to equip them with interfacial properties to allow surface binding and stabilization of the PFC nanoemulsions. We used the FM@PFC nanoemulsion for siRNA lung delivery and found that it showed more potent gene-silencing ability than all the emulsion-free controls. We demonstrated that p.d. of the polyplexes inhibited the lung metastasis progression significantly better than the i.v. injection and proposed FM@PFC/siSTAT3 lung delivery as a more efficient strategy for the treatment of lung metastasis.

In conclusion, we developed a dual therapeutic PFC siRNA nanoemulsion for combined inhibition of CXCR4 and STAT3 by p.d. and achieved increased survival in the established lung metastasis model of advanced breast cancer. The developed nanoemulsions inhibited the proliferation and promoted apoptosis of the metastatic tumors, prevented tumor neovascularization, and activated the immune system. The nanoemulsions administered by pulmonary route could be promising treatments of lung metastasis of varying origins, including advanced osteosarcoma, colorectal cancer, and renal cell carcinoma, which show high probability of lung metastasis and involvement of CXCR4 and STAT3.

MATERIALS AND METHODS

Materials

Heptafluorobutyric anhydride (HFBA) and *N,N'*-hexamethylenebisacrylamide (HMBA) were from Sigma-Aldrich. AMD3100 was purchased from Biochempartner (Shanghai, China). Perfluorodecalin was from Bailingwei Tech (Beijing, China). CXCL12 was from PeproTech (USA). All siRNA (siScr, sense strand, 5′-UUC UCC GAA CGU GUC ACG UTT-3′; siLuc, sense strand, 5′-GGA CGA GGA CGA GCA CUU CUU-3′; siSTAT3, sense strand, 5′-GGU CAA AUU UCC UGA GUU GUU-3′; fluorescein (FAM)- and Cy5-labeled siScr) were from GenePharma (Shanghai, China). DAPI LysoTracker Red and Luciferase Assay Kit were from the Beyotime Institute of Biotechnology. Monoclonal antibodies (β-actin, p-STAT3, STAT3, Bcl-2, pERK, E-cadherin), anti-rabbit immunoglobulin G (IgG), and horseradish peroxidase (HRP)-linked antibody were from Cell Signaling Technology. Annexin V-fluorescein isothiocyanate (FITC)/propidium iodide (PI) kit was from Vazyme Biotech (Nanjing, China). Trypsin, penicillin, streptomycin, RPMI-1640, PBS, and fetal bovine serum (FBS) were from GIBCO (Thermo Fisher Scientific, USA). Human osteosarcoma U2OS cell line expressing EGFP-CXCR4 were from Fisher Scientific. The cells were maintained in DMEM with 2 mM L-glutamine, 1% Pen-Strep, 0.5 mg/mL G418, and 10% FBS. Mouse breast carcinoma 4T1.Luc were from PerkinElmer and cultured in RPMI supplemented with 10% FBS. All the cells were maintained at 37°C and 5% CO_2. Unless otherwise stated, all other reagents were bought from Nanjing Wanqing Chemical Glassware Instrument.

Synthesis of FM and Preparation of FM@PFC

M was synthesized by Michael addition of equimolar ratio of HMBA and AMD3100 as previously reported.[28,47] Then, M was dissolved in 2 mL methanol and mixed with methanol solution of HFBA. Triethylamine was added and the reaction was stirred at room temperature in nitrogen atmosphere and in the dark for 48 h. The mixture was diluted into water (pH 3, HCl) and dialyzed (molecular weight cut-off [MWCO] 3.5 kDa) against water for 2 days before lyophilization to obtain FM. The fluorine content was determined by the elemental analysis (Center of Modern Analysis, Nanjing University, China). The FM@PFC was prepared using the method as previously reported.[26] Briefly, FM (5 mg) was dissolved in diethyl pyrocarbonate-treated water (2 mL) and 20 μL PFC was added. The mixture was sonicated twice with a probe-type sonicator (35% amplitude,

1.5 s power on, 2 s power off) for 35 min in ice-water bath and refrigerated until use.

Preparation and Characterization of siRNA Complexes

The complexes were prepared by adding M, FM, or FM@PFC to the solution of siRNA in HEPES (10 mM, pH 7.4) to achieve the final siRNA concentration of 20 μg/mL. Binding of siRNA was evaluated by 1% agarose gel electrophoresis (100 V, 15 min, JelRed) using formulations prepared at M/siRNA w/w ratios 0–5. Zeta Plus (Zetasizer Nano S90, Malvern) was used to measure size and zeta potential. Particle morphology was determined by TEM (H-600, Hitachi, Japan).

Cytotoxicity

Cytotoxicity was evaluated by 3-(4,5-dimethylthiazol-2-yl)-2,5-diphenyltetrazolium bromide (MTT) assay in L929 cells (1×10^4 cells per well, 96-well plates, cultured for 18 h). Tested polymers and formulations were added and the cells were incubated in 37°C for 24 h. MTT solution (5 mg/mL) was added for another 4 h incubation. Then, DMSO was added and absorbance (490 nm) was measured. Cell viability was analyzed by the GraphPad Prism 6.

Cellular Association and Trafficking

Cell association was measured by flow cytometry in 4T1.Luc cells cultured in 12-well plates. The cells were incubated for 4 h with polyplexes and nanoemulsions were prepared with FAM-siRNA. Then the cells were trypsinized for flow cytometry analysis. The 4T1.Luc cells were treated with FAM-siRNA containing formulations for 1, 3, and 6 h and stained with LysoTracker Red for 45 min before confocal microscopy imaging. Images were analyzed and quantified with ImageJ and GraphPad Prism 6.

Reporter Gene Silencing *In Vitro*

4T1.Luc cells were plated in a 48-well plate at 4×10^4 cells/well and kept overnight. Polyplexes and nanoemulsions (w/w = 2, 100 nM siRNA) prepared with siLuc or siScr were added to the wells for 4 h incubation, and the incubation media was replaced with fresh media with 10% FBS for 24 h incubation. Then, the cells were washed with PBS and lysed with cell lysis buffer. The Luc activity was measured with a commercial assay kit.

Anticancer Activity *In Vitro*

Cancer cell killing activity of the polyplexes was measured by colony formation, MTT, and apoptosis assays. In the colony formation assay, 2,000 cells were added to the cell culture dish and treated with the siSTAT3 polyplexes. After about 10 days incubation, the formed clones were washed with PBS and fixed with 4% polyformaldehyde. After dyeing with Crystal Violet, the clones were photographed and quantified. In the MTT assay, 4T1.Luc cells were seeded in 96-well plates and incubated with siSTAT3 polyplexes for 48 h before measuring cell viability as above. In the apoptosis assay, 4T1.Luc cells were seeded in 12-well plates and treated with the siSTAT3 polyplexes (100 nM) for 48 h incubation. The cells were collected and apoptosis was determined using Annexin V-FITC/PI assay kit (Vazyme Biotech) on BD FACS Calibur flow cytometer. The results were analyzed using FlowJo software (Treestar, USA).

Inhibition of Cancer Cell Invasion and Migration

The transwell invasion assay was performed as previously reported.[24] Briefly, 35 μL ice-cold diluted Matrigel was added to the porous transwell inserts for gelation. U2OS cells were resuspended in serum-free medium containing AMD3100 (300 nM), M, FM, or FM@PFC (M concentration 2.5 μg/mL) for 30 min and added to the inserts. Then, the inserts were placed in a 24-well plate with 20 nM CXCL12 in serum-free medium and incubated at 37°C for 18 h before staining with 0.2% Crystal Violet. The transwell invasion assay of 4T1.Luc cells was performed as above for 48 h except treated with the polyplexes (siSTAT3 100 nM, w/w = 2) and using 10% FBS as a chemoattractant.

Western Blot

The 4T1.Luc cells (5×10^6) were seeded into 6-well plate and incubated overnight. The cells were washed with PBS and the transfection procedure with siSTAT3 (100 nM) polyplexes (w/w = 2) was performed as described above. After 48 h, total protein was extracted and separated by SDS-PAGE followed by transfer to nitrocellulose membrane, probing with Bcl-2, pERK, E-cadherin, p-STAT3, and STAT3 antibodies, and final incubation with HRP-linked secondary antibody at 37°C for 1 h (β-actin was used as a housekeeping control). The band intensities were quantified by ImageJ.

Biodistribution

Mice with 4T1.Luc lung metastases were given a single dose of the polyplexes or nanoemulsions prepared with siScr-Cy5 (1.2 mg/kg siRNA, w/w = 2) by intratracheal instillation or tail vein injection. Fluorescence imaging (exc/em 640/680 nm) was done on IVIS Lumina (Xenogen, USA). Images were acquired 1–24 h after administration. The amount of siScr-Cy5 in tissues was analyzed with IVIS Living Imaging Software.

In Vivo Therapeutic Efficacy

All animal experiments followed regulations of the Institutional Animal Care and Use Committee of China Pharmaceutical University and protocols approved by the Science and Technology Department of Jiangsu Province. A total of 45 female BALB/c mice (8 weeks old) were randomly assigned into five groups with nine animals per group. Half a million 4T1.Luc cells were i.v. injected via tail vein in 100 μL PBS. Treatments were administered either by p.d. or by tail-vein injection on days 7, 9, 11, and 13 for a total of four doses. In the p.d., the mice were anaesthetized and the formulations (w/w = 2) were given in a volume of 40 μL in PBS by intratracheal instillation. Each mouse received 1.2 mg/kg siRNA. On day 15, three mice from each group were randomly selected, injected intraperitoneally with 3 mg of D-luciferin in 100 μL PBS, and sacrificed after 5 min. The lungs were harvested, washed with PBS, and imaged *ex vivo* for Luc expression. The remaining six mice in each group were given two more doses of the treatments on days 15 and 17 and monitored for survival until day 50.

Histopathology

Histopathological analysis was mainly performed by Wuhan Servicebio Technology. Briefly, lung tissues were fixed for 24 h in 4% paraformaldehyde, embedded in paraffin, and sectioned for H&E staining accordingly. For immunohistochemistry staining, the sections were incubated with (p-)STAT3, MMP-9 and Ki67 antibody, and HRP-labeled secondary antibody before analysis with the Vectastain ABC Kit. For immunofluorescence staining, the sections were incubated with anti-CD31, anti-VEGF, anti-CD8, anti-PD-L1, anti-IFN-γ, anti-IL-12, and anti-Foxp3 antibodies. Slides were mounted with Vectashield mounting media containing 4',6-diamidine-2'-phenylindole dihydrochloride (DAPI) before analyzed under fluorescence microscope.

Statistical Analysis

Results are shown as mean ± SD. The Student's t test was used to determine the statistical significance of the differences between two groups and ANOVA for differences among multiple groups. All statistical analyses were performed with GraphPad Prism v6.

SUPPLEMENTAL INFORMATION

Supplemental Information can be found online at https://doi.org/10.1016/j.ymthe.2019.08.008.

AUTHOR CONTRIBUTIONS

Concept and design, D.O., J.L., K.W., and Z.L.; Experimental operation, Z.L., G.C., L.D., Y.W., and C.Z.; Data processing, Z.L., G.C., Y.W., and D.O.; Writing and revision, Z.L., D.O., M.S., and J.L.

CONFLICTS OF INTEREST

D.O. and J.L. are inventors on a patent application related to this work and cofounders of Bohemica Pharmaceuticals, LLC. The remaining authors declare no competing interests.

ACKNOWLEDGMENTS

This work was supported by the National Key Research and Development Program of China (grant number 2017YFA0205400), Science Fund for Distinguished Young Scholars of Jiangsu Province, China (grant number BK20170028), China National Science Foundation (81573377 and 81872817), Changjiang Scholar program, and a start-up from the University of Nebraska Medical Center.

REFERENCES

1. Eckhardt, B.L., Francis, P.A., Parker, B.S., and Anderson, R.L. (2012). Strategies for the discovery and development of therapies for metastatic breast cancer. Nat. Rev. Drug Discov. *11*, 479–497.
2. Jemal, A., Siegel, R., Ward, E., Hao, Y., Xu, J., and Thun, M.J. (2009). Cancer statistics, 2009. CA Cancer J. Clin. *59*, 225–249.
3. Dishop, M.K., and Kuruvilla, S. (2008). Primary and metastatic lung tumors in the pediatric population: a review and 25-year experience at a large children's hospital. Arch. Pathol. Lab. Med. *132*, 1079–1103.
4. Remark, R., Alifano, M., Cremer, I., Lupo, A., Dieu-Nosjean, M.C., Riquet, M., Crozet, L., Ouakrim, H., Goc, J., Cazes, A., et al. (2013). Characteristics and clinical impacts of the immune environments in colorectal and renal cell carcinoma lung metastases: influence of tumor origin. Clin. Cancer Res. *19*, 4079–4091.
5. Heaton, T.E., and Davidoff, A.M. (2016). Surgical treatment of pulmonary metastases in pediatric solid tumors. Semin. Pediatr. Surg. *25*, 311–317.
6. Mansour, H.M., Rhee, Y.S., and Wu, X. (2009). Nanomedicine in pulmonary delivery. Int. J. Nanomedicine *4*, 299–319.
7. Merkel, O.M., Rubinstein, I., and Kissel, T. (2014). siRNA delivery to the lung: what's new? Adv. Drug Deliv. Rev. *75*, 112–128.
8. Xu, C., Wang, P., Zhang, J., Tian, H., Park, K., and Chen, X. (2015). Pulmonary Codelivery of Doxorubicin and siRNA by pH-Sensitive Nanoparticles for Therapy of Metastatic Lung Cancer. Small *11*, 4321–4333.
9. Shim, G., Choi, H.W., Lee, S., Choi, J., Yu, Y.H., Park, D.E., Choi, Y., Kim, C.W., and Oh, Y.K. (2013). Enhanced intrapulmonary delivery of anticancer siRNA for lung cancer therapy using cationic ethylphosphocholine-based nanolipoplexes. Mol. Ther. *21*, 816–824.
10. Balkwill, F.R. (2012). The chemokine system and cancer. J. Pathol. *226*, 148–157.
11. Large, D.E., Soucy, J.R., Hebert, J., and Auguste, D.T. (2019). Advances in Receptor-Mediated, Tumor-Targeted Drug Delivery. Adv. Ther. *2*, 1800091.
12. Zlotnik, A., Burkhardt, A.M., and Homey, B. (2011). Homeostatic chemokine receptors and organ-specific metastasis. Nat. Rev. Immunol. *11*, 597–606.
13. Rhodes, L.V., Short, S.P., Neel, N.F., Salvo, V.A., Zhu, Y., Elliott, S., Wei, Y., Yu, D., Sun, M., Muir, S.E., et al. (2011). Cytokine receptor CXCR4 mediates estrogen-independent tumorigenesis, metastasis, and resistance to endocrine therapy in human breast cancer. Cancer Res. *71*, 603–613.
14. Chen, I.X., Chauhan, V.P., Posada, J., Ng, M.R., Wu, M.W., Adstamongkonkul, P., Huang, P., Lindeman, N., Langer, R., and Jain, R.K. (2019). Blocking CXCR4 alleviates desmoplasia, increases T-lymphocyte infiltration, and improves immunotherapy in metastatic breast cancer. Proc. Natl. Acad. Sci. USA *116*, 4558–4566.
15. Sledge, G.W. (2019). Targeting CXCR4-induced desmoplasia to improve checkpoint inhibition in breast cancer. Proc. Natl. Acad. Sci. USA *116*, 4769–4771.
16. Zorn, E., Nelson, E.A., Mohseni, M., Porcheray, F., Kim, H., Litsa, D., Bellucci, R., Raderschall, E., Canning, C., Soiffer, R.J., et al. (2006). IL-2 regulates FOXP3 expression in human CD4+CD25+ regulatory T cells through a STAT-dependent mechanism and induces the expansion of these cells in vivo. Blood *108*, 1571–1579.
17. Harris, T.J., Grosso, J.F., Yen, H.R., Xin, H., Kortylewski, M., Albesiano, E., Hipkiss, E.L., Getnet, D., Goldberg, M.V., Maris, C.H., et al. (2007). Cutting edge: An in vivo requirement for STAT3 signaling in TH17 development and TH17-dependent autoimmunity. J. Immunol. *179*, 4313–4317.
18. Yu, H., Pardoll, D., and Jove, R. (2009). STATs in cancer inflammation and immunity: a leading role for STAT3. Nat. Rev. Cancer *9*, 798–809.
19. Kujawski, M., Kortylewski, M., Lee, H., Herrmann, A., Kay, H., and Yu, H. (2008). Stat3 mediates myeloid cell-dependent tumor angiogenesis in mice. J. Clin. Invest. *118*, 3367–3377.
20. Yu, H., and Jove, R. (2004). The STATs of cancer–new molecular targets come of age. Nat. Rev. Cancer *4*, 97–105.
21. Yu, H., Kortylewski, M., and Pardoll, D. (2007). Crosstalk between cancer and immune cells: role of STAT3 in the tumour microenvironment. Nat. Rev. Immunol. *7*, 41–51.
22. Jing, N., and Tweardy, D.J. (2005). Targeting Stat3 in cancer therapy. Anticancer Drugs *16*, 601–607.
23. Turkson, J., and Jove, R. (2000). STAT proteins: novel molecular targets for cancer drug discovery. Oncogene *19*, 6613–6626.
24. Chen, G., Wang, Y., Wu, P., Zhou, Y., Yu, F., Zhu, C., Li, Z., Hang, Y., Wang, K., Li, J., et al. (2018). Reversibly Stabilized Polycation Nanoparticles for Combination Treatment of Early- and Late-Stage Metastatic Breast Cancer. ACS Nano *12*, 6620–6636.
25. Chen, G., Wang, K., Hu, Q., Ding, L., Yu, F., Zhou, Z., Zhou, Y., Li, J., Sun, M., and Oupický, D. (2017). Combining Fluorination and Bioreducibility for Improved siRNA Polyplex Delivery. ACS Appl. Mater. Interfaces *9*, 4457–4466.
26. Li, Z., Shen, Y., Wang, Y., Zhu, L., Zhu, C., Qian, C., Sun, M., and Oupicky, D. (2019). Perfluorocarbon Nanoemulsions for Combined Pulmonary siRNA Treatment of Lung Metastatic Osteosarcoma. Adv. Ther. *2*, 1900039.

27. Wang, Y., Kumar, S., Rachagani, S., Sajja, B.R., Xie, Y., Hang, Y., Jain, M., Li, J., Boska, M.D., Batra, S.K., and Oupický, D. (2016). Polyplex-mediated inhibition of chemokine receptor CXCR4 and chromatin-remodeling enzyme NCOA3 impedes pancreatic cancer progression and metastasis. Biomaterials *101*, 108–120.

28. Li, J., and Oupický, D. (2014). Effect of biodegradability on CXCR4 antagonism, transfection efficacy and antimetastatic activity of polymeric Plerixafor. Biomaterials *35*, 5572–5579.

29. Lin, C., Zhong, Z., Lok, M.C., Jiang, X., Hennink, W.E., Feijen, J., and Engbersen, J.F. (2006). Linear poly(amido amine)s with secondary and tertiary amino groups and variable amounts of disulfide linkages: synthesis and in vitro gene transfer properties. J. Control. Release *116*, 130–137.

30. Niu, G., Heller, R., Catlett-Falcone, R., Coppola, D., Jaroszeski, M., Dalton, W., Jove, R., and Yu, H. (1999). Gene therapy with dominant-negative Stat3 suppresses growth of the murine melanoma B16 tumor in vivo. Cancer Res. *59*, 5059–5063.

31. Bassères, D.S., and Baldwin, A.S. (2006). Nuclear factor-kappaB and inhibitor of kappaB kinase pathways in oncogenic initiation and progression. Oncogene *25*, 6817–6830.

32. Wang, T., Niu, G., Kortylewski, M., Burdelya, L., Shain, K., Zhang, S., Bhattacharya, R., Gabrilovich, D., Heller, R., Coppola, D., et al. (2004). Regulation of the innate and adaptive immune responses by Stat-3 signaling in tumor cells. Nat. Med. *10*, 48–54.

33. Fontenot, J.D., Gavin, M.A., and Rudensky, A.Y. (2003). Foxp3 programs the development and function of CD4+CD25+ regulatory T cells. Nat. Immunol. *4*, 330–336.

34. Hori, S., Nomura, T., and Sakaguchi, S. (2003). Control of regulatory T cell development by the transcription factor Foxp3. Science *299*, 1057–1061.

35. van Kempen, L.C., and Coussens, L.M. (2002). MMP9 potentiates pulmonary metastasis formation. Cancer Cell *2*, 251–252.

36. Hiratsuka, S., Nakamura, K., Iwai, S., Murakami, M., Itoh, T., Kijima, H., Shipley, J.M., Senior, R.M., and Shibuya, M. (2002). MMP9 induction by vascular endothelial growth factor receptor-1 is involved in lung-specific metastasis. Cancer Cell *2*, 289–300.

37. Esposito, C.L., Nuzzo, S., Catuogno, S., Romano, S., de Nigris, F., and de Franciscis, V. (2018). STAT3 Gene Silencing by Aptamer-siRNA Chimera as Selective Therapeutic for Glioblastoma. Mol. Ther. Nucleic Acids *10*, 398–411.

38. Yoon, S., Wu, X., Armstrong, B., Habib, N., and Rossi, J.J. (2019). An RNA Aptamer Targeting the Receptor Tyrosine Kinase PDGFRα Induces Anti-tumor Effects through STAT3 and p53 in Glioblastoma. Mol. Ther. Nucleic Acids *14*, 131–141.

39. Fujita, Y., Yagishita, S., Hagiwara, K., Yoshioka, Y., Kosaka, N., Takeshita, F., Fujiwara, T., Tsuta, K., Nokihara, H., Tamura, T., et al. (2015). The clinical relevance of the miR-197/CKS1B/STAT3-mediated PD-L1 network in chemoresistant non-small-cell lung cancer. Mol. Ther. *23*, 717–727.

40. Chen, J., Jiang, C.C., Jin, L., and Zhang, X.D. (2016). Regulation of PD-L1: a novel role of pro-survival signalling in cancer. Ann. Oncol. *27*, 409–416.

41. Voorwerk, L., Slagter, M., Horlings, H.M., Sikorska, K., van de Vijver, K.K., de Maaker, M., Nederlof, I., Kluin, R.J.C., Warren, S., Ong, S., et al. (2019). Immune induction strategies in metastatic triple-negative breast cancer to enhance the sensitivity to PD-1 blockade: the TONIC trial. Nat. Med. *25*, 920–928.

42. Wang, C., Sun, W., Ye, Y., Hu, Q., Bomba, H.N., and Gu, Z. (2017). In situ activation of platelets with checkpoint inhibitors for post-surgical cancer immunotherapy. Nat. Biomed. Eng. *1*, 0011.

43. Yu, P., Han, X., Yin, L., Hui, K., Guo, Y., Yuan, A., Hu, Y., and Wu, J. (2019). Artificial Red Blood Cells Constructed by Replacing Heme with Perfluorodecalin for Hypoxia-Induced Radioresistance. Adv. Ther. *2*, 1900031.

44. Zhuang, J., Ying, M., Spiekermann, K., Holay, M., Zhang, Y., Chen, F., Gong, H., Lee, J.H., Gao, W., Fang, R.H., and Zhang, L. (2018). Biomimetic Nanoemulsions for Oxygen Delivery In Vivo. Adv. Mater. *30*, e1804693.

45. Liberman, A., Wang, J., Lu, N., Viveros, R.D., Allen, C.A., Mattrey, R.F., Blair, S.L., Trogler, W.C., Kim, M.J., and Kummel, A.C. (2015). Mechanically Tunable Hollow Silica Ultrathin Nanoshells for Ultrasound Contrast Agents. Adv. Funct. Mater. *25*, 4049–4057.

46. Matsumoto, S., and Kuroda, Y. (2002). Perfluorocarbon for organ preservation before transplantation. Transplantation *74*, 1804–1809.

47. Li, J., Zhu, Y., Hazeldine, S.T., Li, C., and Oupický, D. (2012). Dual-function CXCR4 antagonist polyplexes to deliver gene therapy and inhibit cancer cell invasion. Angew. Chem. Int. Ed. Engl. *51*, 8740–8743.